

L I C E N C E T O M c M A S T E R U N I V E R S I T Y

This Thesis has been written
[Thesis, Project Report, etc.]

by William Paul Chawrun for
[Full Name(s)]

Undergraduate course number 4K6 at McMaster
University under the supervision/direction of _____
Dr. D. M. Shaw

In the interest of furthering teaching and research, I/we
hereby grant to McMaster University:

1. The ownership of 3 copy(ies) of this work;
2. A non-exclusive licence to make copies of this work, (or any part thereof) the copyright of which is vested in me/us, for the full term of the copyright, or for so long as may be legally permitted. Such copies shall only be made in response to a written request from the Library or any University or similar institution.

I/we further acknowledge that this work (or a surrogate copy thereof) may be consulted without restriction by any interested person.

David Shaw
Signature of Witness,
Supervisor

Paul Chawrun
Signature of Student

April 27th 1988
date

THE BORON PARTITION AMONG COEXISTING MINERALS IN
SOME IGNEOUS AND METAMORPHIC ROCKS

THE BORON PARTITION AMONG COEXISTING MINERALS IN SOME
IGNEOUS AND METAMORPHIC ROCKS

BY:

W. PAUL CHAWRUN

Submitted to the Department of Geology
in Partial Fulfilment of the Requirements
for the degree
Bachelor of Science

April, 1988

BACHELOR OF SCIENCE (1988)
(Geology)

McMASTER UNIVERSITY
Hamilton, Ontario

TITLE: The boron partition among coexisting minerals in
 some igneous and metamorphic rocks.

AUTHOR: William Paul Chawrun

SUPERVISOR: Denis M. Shaw

NUMBER OF PAGES: i - viii; 1 - 39

ABSTRACT

Separated minerals from 18 different rock samples were available. These came from various locations in the Grenville province. Of these samples, there were 44 minerals which had at least one coexisting mineral phase. These were all analysed for boron by thermal neutron irradiation using the Prompt Gamma Neutron Activation Analysis at McMaster University Nuclear Reactor. There was a preferential boron partition determined for the samples originating from an igneous source, and a numerical value of 0.7 was determined for K-feldspar/Biotite. There was no preferential boron partition among the coexisting phases that originated from a metamorphic source. Sphene and fluorite contained much less boron than other minerals that coexisted with them.

ACKNOWLEDGEMENTS

I would like to thank Dr. D.M. Shaw for his suggestion of this topic, for his guidance and patience during the investigation and for the use of his samples, without which this study would not have been possible. I would also like to thank Dr. M.G. Truscott for her assistance with the PGNAA, Arun Sen for his assistance with the plotting of the graphs, and Patty Smith for her help in determining the precision of the PGNAA system.

I would also like to thank Ray Ruckpaul, Jim Robertson and the rest of the regulars in room 119A for their moral support during the stressful weeks before completion of this project.

TABLE OF CONTENTS

	PAGE
CHAPTER 1 INTRODUCTION	1
CHAPTER 2 PREVIOUS WORK	2
2.1 Trace Element Substitution Into Crystal Lattices	2
2.2 Trace Element Behavior During Metamorphism	3
2.3 The Nernst Partition Law	3
2.4 The Distribution Coefficient	5
2.5 The Behavior of Boron	7
2.6 Previous Studies on the Occurrence of Boron in Minerals	7
CHAPTER 3 DESCRIPTION OF THE SAMPLES	10
3.1 Origin	10
3.2 Purity of the Samples	11
CHAPTER 4 METHOD OF ANALYSIS	16
4.1 Introduction	16
4.2 The PGNA A System at McMaster University	17
4.3 Preparation of the Samples	18
4.4 Calibration of PGNA A	21
4.5 Analysis of the Boron Peak	21
4.5.1 Sodium Interference	22
4.5.2 Sodium Correction	22
4.6 Calculation of Boron Concentration	22

	PAGE
4.7 The Blank Interference	24
4.8 Precision of PGNA	25
4.9 Accuracy of PGNA	25
CHAPTER 5 INTERPRETATIONS	
5.1 Discussion of the Results	28
5.2 Comparisons and Interpretations	36
5.3 Summary	37
REFERENCES	39

LIST OF TABLES

TABLE		PAGE
3.1	Description of the Samples	13
3.2	The Purity of the Samples	14-15
4.1	Boron Analysis of NBS-1571	27
5.1	The Measured Boron Concentrations of the Samples	29-30
5.2	The Distribution Coefficients of Coexisting Minerals	31

LIST OF FIGURES

FIGURE	PAGE
4.1 Cross-Section of the Beam Port	17
4.2 The Beam Port "cave"	18
4.3 The Prompt Gamma Peaks of Sodium and Boron	23
5.1 Plagioclase vs. Biotite	32
5.2 Hornblende vs. Biotite	33
5.3 Biotite vs. K-Feldspar	34

CHAPTER ONE

INTRODUCTION

Trace element distribution between coexisting mineral phases has been studied extensively by many people since the early 1950's. The objective of this project is to find a preferential boron partition among coexisting minerals from igneous and metamorphic rocks. Recently a similar study has been made by E. Gray et al. to find the preferential boron and lithium partition in high grade rocks and minerals. Since their results were puzzling and ambiguous, they concluded that more work needed to be done on this subject.

This project used samples that were collected by different people from various locations in the Grenville province of the Canadian Shield in Ontario and Quebec, including both igneous and metamorphic rocks.

CHAPTER TWO

PREVIOUS WORK

2.1 Trace Element Substitution Into Crystal Lattices

The concept of trace element substitution into a crystal lattice has been intensely researched by many authors since the early 1950's. One of the first breakthroughs in this field of science was by V.M. Goldschmidt, when he developed rules as a guide for the distribution of elements during magmatic crystallization. When an element is incorporated into a crystal lattice, Goldschmidt (1937,1944) in Taylor, S.R. (1965), said it is "admitted", "camouflaged", or "captured" depending on the relationship between the ionic radius and charge of the element with that of the crystal lattice. Later, Shaw (1953,p.146) stated that "it cannot be predicted whether a trace element will be concentrated in early or late mineral fractions on the basis of ionic radii". Through this, it was discovered that the nature of the chemical bond had to be considered as well as the ionic valency. Ringwood (1955a,b) used electronegativity as a measurement of bond type and drew attention to the weakening effect of partial covalency on the bond strength of metal oxides. He determined this by performing experiments to find relative melting point data for oxide minerals that have similar structures. Ringwood made another important discovery by finding that highly charged cations tend to form complexes in magmas, usually occurring with oxygen or hydroxyl anions. Due to all of this, it has been determined that the probability that an element

will form a complex can be found by determining its ratio of ionic charge to ionic radius, or the ionic potential. It has been found that elements that have high ionic potentials usually form complexes in magmas. In general, the behavior of a minor element incorporating into a crystal lattice is based on the elements ionic size, its valency and the type of chemical bond that is produced in the crystal lattice.

2.2 Trace Element Behavior During Metamorphism

When a rock is subjected to severe temperature and pressure conditions the elements change coordination and position in relation to each other. As a result, the rock may undergo recrystallization. When trying to understand the effect of metamorphism on the distribution of trace elements in a rock, element migration must be considered. One of the most important discoveries in this field was by Shaw (1954) who carried out studies on pelitic rocks of the Littleton formation. These rocks show increasing metamorphic grade, and trace element data were collected over varying facies. It was found that the concentration of most of the elements remained constant throughout varying degrees of metamorphism.

2.3 The Nernst Partition Law

Trace element distribution between coexisting minerals, under ideal conditions, is governed by thermodynamic principles (Mason 1982). On the basis of thermodynamic equilibrium, the

pattern of trace element distribution can be used to try to find the conditions of metamorphism. The Nernst Partition Law governs the distribution of a trace element between two coexisting phases, and is explained in the following derivation.

Consider the following equation:

$$u_i^\alpha = u_i^{\circ\alpha} + RT \ln x_i^\alpha \gamma_i^\alpha$$

$$u_i^\beta = u_i^{\circ\beta} + RT \ln x_i^\beta \gamma_i^\beta$$

Where u_i^α and u_i^β are the chemical potentials of component i in phases α and β ; $u_i^{\circ\alpha}$ and $u_i^{\circ\beta}$ denote the chemical potentials of component i at unit activity and x_i^α , x_i^β and γ_i^α , γ_i^β denote the mole fractions and activity coefficients of component i in phases α and β , respectively.

At equilibrium, the chemical potentials between two coexisting phases are equal, so:

$$u_i^\alpha = u_i^\beta$$

thus:

$$u_i^{\circ\alpha} + RT \ln x_i^\alpha \gamma_i^\alpha = u_i^{\circ\beta} + RT \ln x_i^\beta \gamma_i^\beta$$

let:

$$u_i^{\circ\alpha} - u_i^{\circ\beta} = \Delta G_i^\circ$$

$$\text{then: } RT \ln \frac{x_i^\beta \gamma_i^\beta}{x_i^\alpha \gamma_i^\alpha} = -\Delta G_i^\circ$$

If:

$$\frac{x_i^\beta \gamma_i^\beta}{x_i^\alpha \gamma_i^\alpha} = K_i$$

Where K_i is the equilibrium constant of the system, then:

$$\ln K_i = - \frac{\Delta G_i^0}{RT}$$

If we assume that the two phases are ideal mixtures, then the activity coefficients can be stated as:

$$\gamma_i^\beta = \gamma_i^\alpha = 1$$

so that:

$$\frac{x_i^\alpha}{x_i^\beta} = K_i$$

It can be seen that the equilibrium constant, K_i , is dependent upon the temperature of the system. Also, K_i is a ratio between two molar concentrations. In practice, the ratio of the two concentrations of component i in phases α and β is used instead of the ratio of the two molar concentrations of component i in those phases. The partition coefficient K_i is then written as K_D , so that:

$$K_D = c_i^\alpha / c_i^\beta$$

This is the usual form of the Nernst partition law. K_D is the distribution coefficient for component i in phases α and β , and c is the concentration of component i in those phases by weight.

It was previously thought that the Nernst distribution law only applied to trace components which mixed ideally, however recent studies have shown that this is not always the case.

2.4 The Distribution Coefficient

The distribution of a trace element between pairs of

coexisting minerals can be expressed when two concentrations of a component i are plotted against each other. This is called a distribution diagram and each point represents one mineral pair. For trace element concentrations in crystal lattices, it follows Nernst's partition law that if a straight line is produced, the system is in equilibrium and both minerals are ideal solutions for this component. However, perfectly ideal conditions are unlikely in nature, due to the crystal lattices usually containing defects and impurities. Due to this, the distribution plot approaches a straight line if there is in fact a preferential partition between the two mineral phases, and a best fit line is drawn to determine the partition coefficient.

The charge on a crystal lattice system must be constant overall, with both positive and negative charges isolated within it, counteracting each other. During ideal mixing of two mineral phases, deviations in the distribution coefficient can be expected when ions that have a different charge substitute into structural sites within the lattice. For example, this might occur if a $[\text{BO}_3]^{3-}$ ion occupied a structural site that was usually occupied by a differently charged ion.

If the plotted points on the distribution diagram are scattered and no best fit line can possibly be drawn, the distribution coefficient's variable plot may have been produced due to the variable concentration of another element in either or both mineral phases. In some cases, a scattered diagram suggests contamination of the minerals. Kretz (1960) discusses the

possibilities of variable distribution coefficients. Also, Kretz (1961) states that the distribution coefficient of an element between two phases is dependant upon the variations in the temperature and pressure of the system.

2.5 The Behavior of Boron

Elements that have high ionic potential tend to form complexes. Boron has a high ionic potential and can exist in three or four fold coordination with oxygen as $[\text{BO}_3]^{3-}$ or $[\text{BO}_4]^{5-}$ complexes. Boron is thought to usually enter silicates as a borate ion, but $[\text{BO}_3]^{3-}$ is not readily accepted into crystal lattices and is usually concentrated in residual magmas. The $[\text{BO}_4]^{5-}$ complex may be expected to replace the $[\text{AlO}_4]^{5-}$ tetrahedra in feldspars, as is shown by reedmergite (NaBSi_3O_8). For an extensive list of all the established mineral borate structures, one is referred to Tennyson (1963) in Christ, C.L., and Harder, H.A.. Tourmaline is the most important boron bearing mineral, with about 9-11.5% B_2O_3 . Since boron is usually enriched in residual melts within a magma, tourmaline is often more concentrated in pegmatites and hydrothermal veins than the average composition of boron in crustal rocks.

2.6 Previous Studies on the Occurrence of Boron in Minerals

Determining of the occurrence of boron in minerals has been studied through alpha-track analysis (Truscott et al 1986) and (Ahmad et al 1981), and through radiographic analysis (Malinko et

al. 1979). With these methods, it is very difficult to distinguish between Lithium and Boron effects. Due to this, some of the results that are thought to be boron effects may actually be due to lithium. The alpha-track analysis shows that boron (or lithium) is very concentrated in sericitic alteration within plagioclase, developed inward from cleavages and boundaries. In general, it has been found that sericitized, saussuritized and chloritized alteration products of biotite, plagioclase and minor mafic minerals have higher boron content than alteration free areas. Boron has also been found to be concentrated along grain boundaries and in cracks in pyroxene, plagioclase and garnet. Truscott et al. report that boron may also be in fluid inclusions within plagioclase, although this has not been proven.

Malinko et al. concluded that their evidence suggested isomorphous entry of boron into crystal lattices. They also concluded that when different concentrations of boron are found within different mineral zones, it means changes in the crystal lattice have occurred during growth. Ahmad and Wilson state that the mobility of boron appears to be related to the presence of a metamorphic fluid phase.

In summary, it has been found that in common metamorphic rocks, alteration minerals such as sericite, saussurite and chlorite contain the richest amount of boron concentration. In non altered rock forming minerals, Truscott et al. found that the boron content in order of decreasing concentration is: biotite > clinopyroxene > orthopyroxene, plagioclase, amphibole, garnet >

perthite, quartz. It is important to keep in mind that the conclusions made in these papers may not be totally due to boron effects, as a method for distinguishing the difference between boron and lithium in alpha-track analysis has not been perfected yet.

CHAPTER THREE

DESCRIPTION OF THE SAMPLES

3.1 Origin

The samples used in this study were collected from various locations in the Grenville province in Ontario and Quebec. The MCC series samples were collected by M.C. Chiang from almandine amphibolite facies rocks (of possible igneous origin) from the Loon Lake Aureole in Chandos Township for his M.Sc thesis (1965). Also from Chandos township are the U-series samples, which were collected by J. Dostal for his Ph.D thesis (1973) from the Loon Lake Pluton. This complex is approximately 36 miles NNE of Peterboro, Ontario. For extensive discussions on the Loon Lake complex, one is referred to Chiang (1965) and Dostal (1973). The U-series samples are of igneous origin, as they are all either monzonites or quartz monzonites. The rest of the samples were collected by D.M. Shaw. The 721104 sample is a gabbro originating from an outcrop on Hwy. 62, 9.6 miles south of Bancroft, Ontario, and the 690422-3 sample is a para-amphibolite originating from an outcrop 1.5 miles west of Gooderham, Glamorgan Township, Haliburton County, Ontario. All of the Ca-series samples originated from Grand Calumet Township, Pontiac County, Quebec, except for Ca-105 which is from Huddersfield Township, Quebec. These rocks are all of metamorphic origin, and are all various types of metamorphosed carbonate rocks of amphibolite grade. The origins of the samples are summarized in table 3.1.

For the procedure of separating the mineral grains from their originating rocks, one is referred to Chiang (1965) or Dostal (1973).

3.2 Purity of the Samples

The samples were examined optically to:

- 1) Determine their purity.
- 2) Find boron containing minerals, such as tourmaline.
- 3) Determine the extent of alteration.

The mineral grains were mounted on a slide and immersed in an oil with a similar index of refraction. A cover slip was then placed on top of the mineral grains and oil. The purpose of surrounding the mineral grains with an oil of similar index of refraction was to make its relief very low. This caused an impurity to be much more conspicuous, as it showed higher or lower relief. Each mineral sample was then counted for purity using a petrographic microscope. A mineral was considered >99% pure if 100 grains were counted without seeing any foreign grains, 99% pure if one was seen, and so on. In some cases, the impure grains were much smaller than the mineral under consideration. When this occurred, the volume difference of the two types of grains was taken into consideration. For example, if a plagioclase sample was found to have a plagioclase:quartz ratio of 9:1, and the quartz grains were half the volume of the plagioclase grains, the sample was said to be 95% pure.

No tourmaline was found in any of the samples. Also, very few grains showed any alteration, and it was minor in the ones

that did.

The results of the mineral examination are presented in Table 3.2.

Table 3.1 Description of the Samples

SAMPLE	ORIGIN	ROCK TYPE
MCC-761 MCC-703 MCC-704	-Loon Lake Aureole, Chandos Twp., Ont.*	-Almandine Amphibolite of possible igneous origin
U-70 U-27 U-94 U-115 U-251 U-26	-Loon Lake Pluton, Chandos Twp., Ont.°	-Diorite -Quartz Monzonite -Monzonite -Quartz Monzonite -Monzonite -Quartz Monzonite
690422-3	-1.5 M west of Gooder- □ ham, Glamorgan twp., Haliburton Co., Ont.	-Para-Amphibolite
721104	-Hwy. 62, 9.6 M south of Bancroft, Ont.	-Gabbro
Ca-30 Ca-44a Ca-56 Ca-76 Ca-65 Ca-105	-Grand Calumet Twp., Δ Pontiac Co., Quebec	-Pegmatitic Skarn -Fluorite Pyroxene Syenite -Skarn -Skarn -Skarn
	-Huddersfield Twp., + Pontiac Co. Quebec	-Uraniferous Diopside Marble
On-10	-Locality Uncertain	

Map References

- * Chaing, M.C., 1965. Page 4 and in the pocket.
- ° Dostal, J., 1973 In the pocket.
- Δ Shaw, D.M., 1958 Page 29 and in the pocket.
- + Shaw, D.M., 1958 Page 37.
- Pacesova, M., 1973 In the pocket

TABLE 3.2 The Purity of the Crushed Mineral Samples

SAMPLE	MINERAL	PURITY	OTHER DISTINGUISHING FEATURES
U-70	Plagioclase Hornblende	99% >99%	-slight saussuritization in a few grains -slight alteration along fracture planes
U-27	Biotite K-Feldspar	>99% >99%	-a few grains have slight inclusions
U-94	Biotite K-Feldspar Plagioclase + Quartz	>99% 98% (82% 15%)	-3% biotite, quartz grains show some minor fluid inclusions
U-115	K-Feldspar Biotite	98% >99%	-2% quartz
U-251	K-Feldspar Biotite Plagioclase + Quartz	98% >99% (80% 20)	
U-26	K-Feldspar Biotite	99% >99%	
MCC-703	Hornblende Biotite	95% 98%	-5% biotite -2% hornblende
MCC-704	Biotite Hornblende	99% >99%	
MCC-761	Biotite Hornblende	99% 95%	-fluid inclusions in 10% of the grains -5% biotite
721104	Biotite Orthopyrx. Opx. + Cpx.	70%	-30% chlorite -It was not possible to distinguish between the two pyroxenes
690422-3	Sphene Hornblende K-Feldspar Plagioclase	99% 99% 99% 98%	-2% quartz
Ca-30	Phlogopite Pyroxene Scapolite + Sphene	>99% >99% (93% 5%)	-a few grains show fluid inclusions -2% plagioclase

(continued...)

TABLE 3.2 Continued

SAMPLE	MINERAL	PURITY	OTHER DISTINGUISHING FEATURES
Ca-44a	Fluorite + Apatite Pyroxene	(>99% <1% 99%	-20% of the grains show inclusions
Ca-105	Phlogopite Diopside	>99% 98%	
ON-10	Biotite Sphene	>99% 97%	
Ca-56	Sphene Pyroxene	99% 99%	-unidentified green pyroxene
Ca-76	Hornblende Sphene	99% 99%	
Ca-65	Fluorite Magnetite + Pyroxene	99% (20% 80%)	

CHAPTER FOUR

METHOD OF ANALYSIS

4.1 Introduction

Until recently, boron geochemistry had not been widely studied due to the usual low abundance of boron in rocks and the lack of analytical methods to measure it. A method enabling one to measure the concentration of boron has been developed, called Prompt Gamma Neutron Activation Analysis (PGNAA). This method is excellent because it is fast, non-destructive and requires minimal sample preparation. PGNAA was used to determine the boron concentration of the samples in this project.

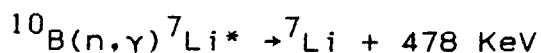
During PGNAA, a crushed sample is irradiated with thermal neutrons that are emitted via a beam port connected to the core of a nuclear reactor. This causes the sample to emit gamma rays which are measured by a detector and multi-channel analyzer (MCA). The concentration of the element is then calculated with reference to a standard of known concentration.

The theory behind PGNAA as a means of measuring minor element concentrations has been discussed in many different publications, including Middleton (1987), Ash (1987, pg 25-38) and Higgins et al. (1984).

An element can be used for PGNAA if it has a large thermal neutron cross-section and undergoes an (n,γ) nuclear reaction when irradiated. Boron is an excellent element to be measured by PGNAA because it shows both of these characteristics.

Each element has its own characteristic prompt gamma energy

level, which is 478 KeV for boron. In the case of boron irradiation, the reaction that occurs is $^{10}\text{B}(n,\gamma)^7\text{Li}^*$. This states that a ^{10}B atom reacts with a neutron to form $^7\text{Li}^*$, which is in an excited state. The decay of $^7\text{Li}^*$ to ^7Li produces the gamma ray that is measured by the MCA. The reaction can also be stated as:



4.2 The PGNAA System at McMaster University

The analyses were carried out at McMaster University Nuclear Reactor in Hamilton, Ontario, located on the McMaster University campus.

The neutrons used for the PGNAA system were extracted from a 2 MW pool-type reactor by use of a beam port, which connects directly to the core. The neutron flux of the reactor is $10^{13} \text{ ncm}^{-2} \text{ s}^{-1}$. Only thermal neutrons are required for PGNAA, but the beam port also carries fast neutrons and gamma rays that might damage the detection system and cause a large gamma-ray background. In order to protect the detection system and filter out the fast neutrons, a combination of 60 cm of cylindrical silicon crystals (12 cm in diameter) and 30 cm of sapphire crystals (7 cm in diameter) are used. Collimators of lead and heavy concrete are used, and then the beam is shaped by a rotatable shutter of polyethylene and lead. Lithium carbonate wax ($^6\text{LiCO}_3$) is used to further reduce the spread of the neutron beam within the system. After filtering, the thermal neutron

flux at the sample position is $6 \times 10^7 \text{ ncm}^{-2}\text{s}^{-1}$ with a Cd ratio >100. (Higgins et al. 1984) See fig. 4.1

The gamma rays emitted by the samples during irradiation are detected by an "n"-type Ortec HPGe co-axial detector (see fig. 4.2), specially made with ^{11}B ion implantation to lessen the effect of ^{10}B background during analysis. The signals emitted by the detector are analyzed by a Canberra Series 85 multi-channel analyzer which displays the output on a computer screen.

4.3 Preparation of Samples

The procedure used for the preparation of samples for PGNA has been described by T.A. Middleton (1987).

Each sample was accurately weighed to three decimal places, with the average weight a little more than one gram. Each was then placed and sealed by two polyethylene caps into a 7 cm by 1 cm teflon tube, with the powder depth not exceeding 2 cm, ensuring it to have maximum exposure to the neutron beam. In some cases, there was very little powder available and consequently the powder depth was less. Each sample was lowered into the beam and suspended by a teflon rod. The optimum distance for the sample to be lowered is 114.0 cm, measured by T.A. Middleton (1987). Some of the tubes were slightly curved and had to be positioned so that all of the sample was irradiated by the beam. Most of the samples were irradiated and counted for 1000 seconds: those richer in boron only needed to be measured for 500 seconds, while those poorer in boron took longer to

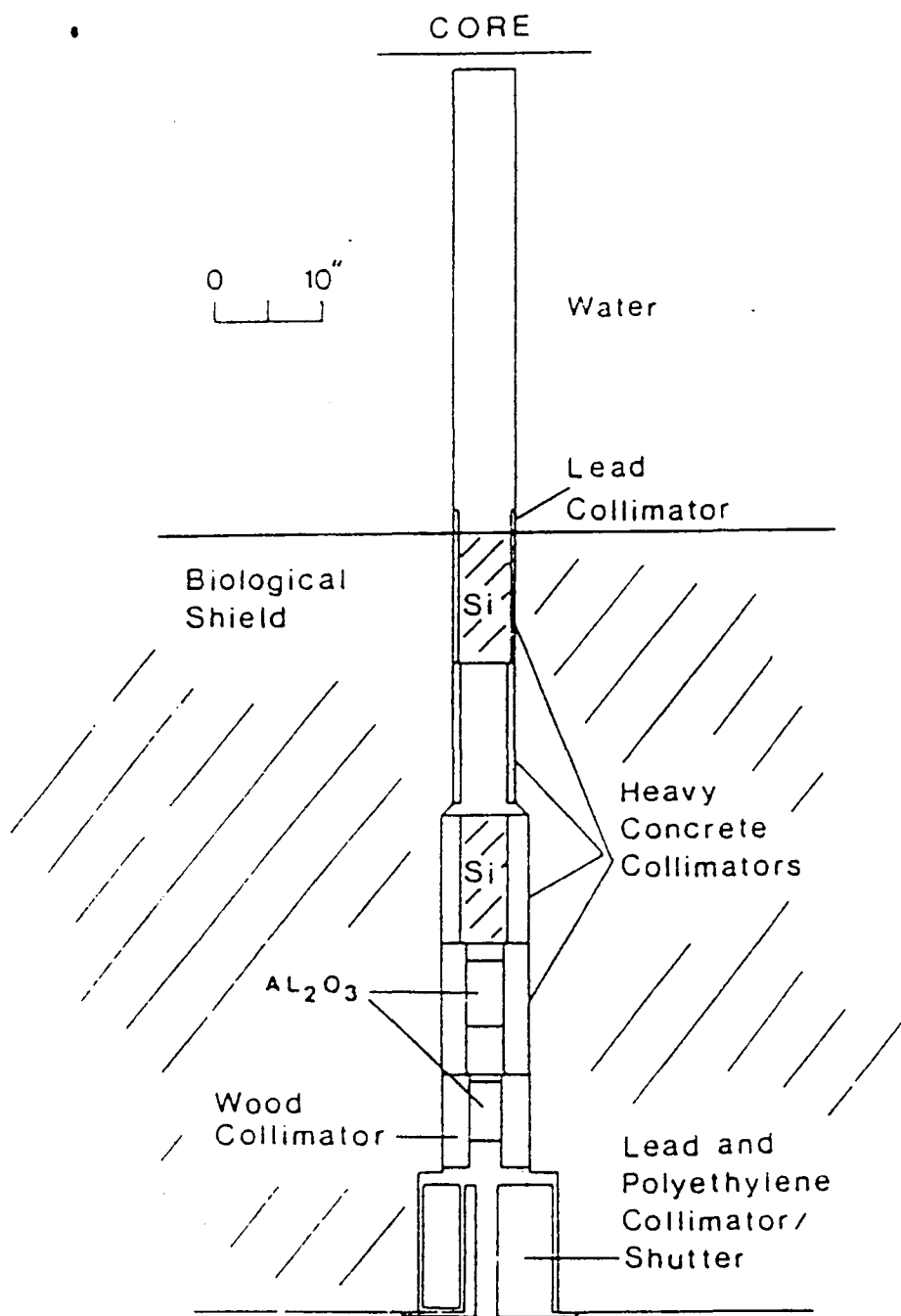


FIGURE 4.1

Cross-section of the beam port. (after Higgins et al., 1984)

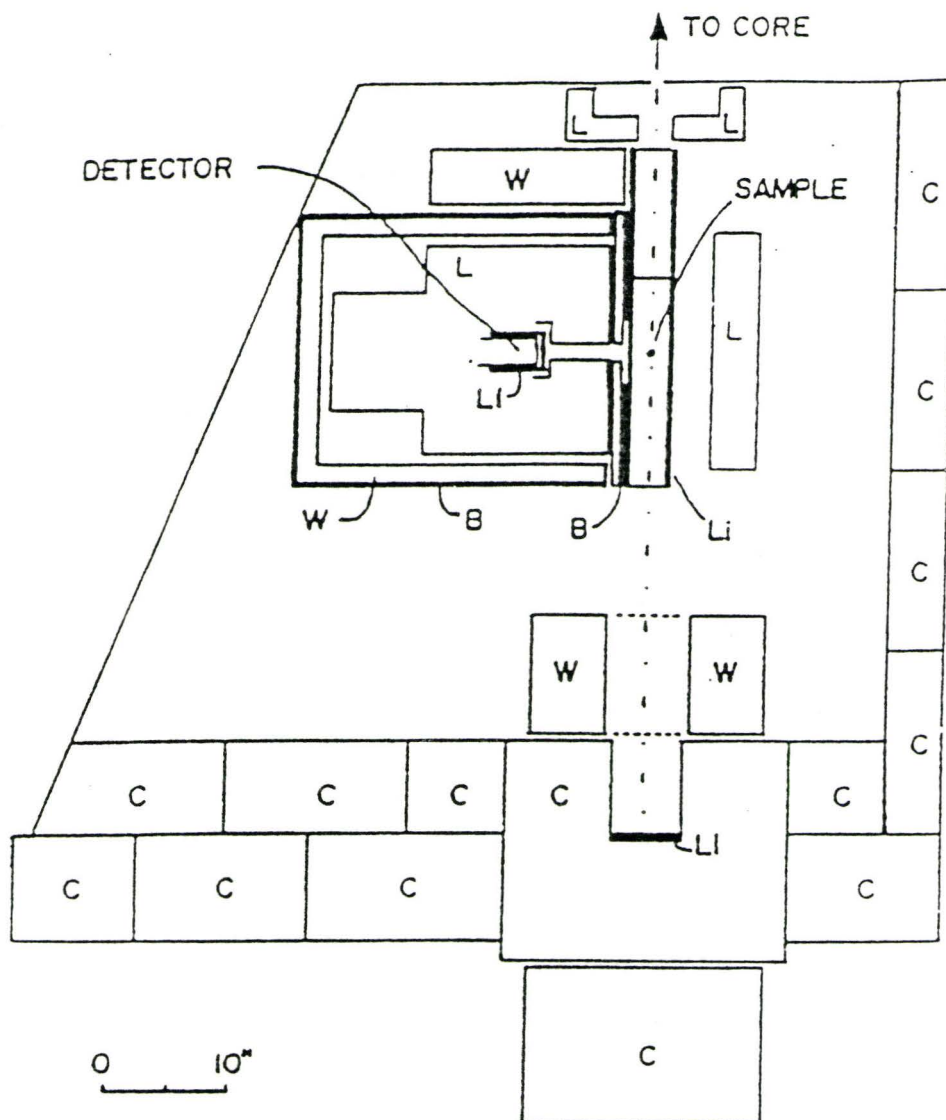


FIGURE 4.2

The neutron beam enters the "cave" at the top of the diagram. Shielding materials are lead (L), wax (X), boraflex (B), $^6\text{LiCO}_3$ in wax (Li) and concrete (C). (after Higgins et al., 1984)

develop a peak and were measured for 2000 seconds.

4.4 Calibration of PGNA

The analysis method was calibrated using standards consisting of materials of known boron concentration.

The synthetic reference standards used was boric acid #B-7, prepared by T.A. Middleton. A 1000 ppm boron stock solution was made by dissolving 0.5179 g of boric acid (H_3BO_3) in 100g of deionized, distilled "Milli-Q" water. Later, a small amount of distilled 16 molar nitric acid (HNO_3) was added (<1ml). The stock solution was then deposited onto precipitated silicic acid ($\text{H}_2\text{SiO}_3 \cdot n\text{H}_2\text{O}$) which forms a rock like matrix and distributes the solution evenly. An Eppendorf pipette was used to deposit 0.102 g of the solution onto the silicic acid matrix which had been previously loaded into the teflon tubes. The tubes were then sealed with polyethylene caps. The standard is reported to contain precisely 102 ug of boron. (Ash 1987)

The standard was run for 1000 seconds before every analysis. Due to possible fluctuations in the reactor flux, the sample needed to be run for every three hour interval.

International reference standards are used to measure the accuracy of the prompt gamma system. The best known boron standard is NBS SRM 1571-Orchard leaves, which has a certified boron value of 33 ± 3 ppm. (Middleton 1987)

4.5 Analysis of the Boron Peak

4.5.1 Sodium Interference

When an element is irradiated with thermal neutrons, it emits gamma rays at its own characteristic prompt gamma energy level. The prompt gamma energy level for sodium is 472 KeV, and is close to the peak for boron. Since the sodium peak is so close to the boron peak, it usually causes interference. The boron peak is wide and flat-topped, whereas the sodium peak is sharp. The net effect is a broad peak with a projection on the left hand side. (See figure 4.3)

4.5.2 Sodium Correction

Sodium is a common constituent of most rock types, so a correction is often necessary. Correction for the sodium peak when calculating the concentration of boron using PGNA has been discussed by Higgins et al. (1984) and Middleton (1987). The method used for correction is called the "partial peak method" (developed by Higgins et al.) and avoids a sodium correction for the calculation afterward. Using this method, the middle of the flat topped peak that has not been interfered with by sodium is used as the total count rate. In fig. 4.3 the total count rate is "a". The values of "b₁" and "b₂" are averaged and subtracted from the count rate determined for "a" to give the total count rate for boron in the sample. The width of "a", "b₁" and "b₂" are each nine channels across, which is equivalent to nine KeV.

4.6 Calculation of Boron Concentration

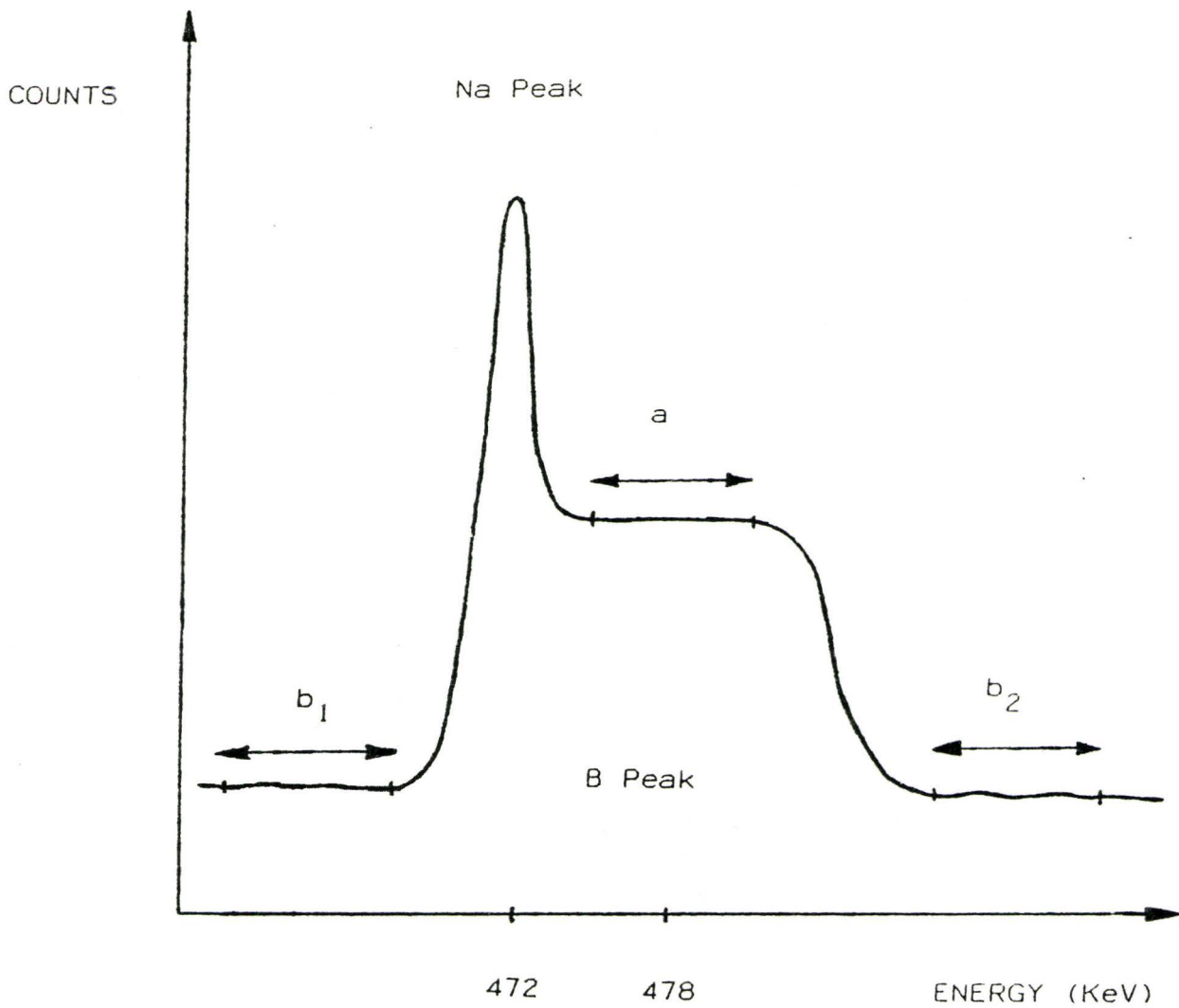


Figure 4.3

The prompt gamma peaks of sodium and boron. Boron concentrations were determined using the partial peak method which involved subtracting the average of both backgrounds (b_1 and b_2) from the total for the boron peak (a). This eliminated the effect of the sodium peak in the calculation. (note: The count rate for b_1 is always higher than for b_2 .)

Once the peak for a sample had been established on the computer screen by the MCA, the partial peak method for calculation of concentration was used. The first step was determining the number of counts per second (ct/s) of the sample by finding the total boron count rate $[(a - (b_1 + b_2))/2]$ in fig. 3.3] and dividing it by the length of time it was irradiated. The ct/s of the standard was calculated the same way, and then divided by it's absolute boron content to give ct/s/ug. The ct/s of the sample was then divided by the ct/s/ug of the standard. Subtracted from this number was the average amount of boron in a blank teflon tube with two polyethylene caps. This number was then divided by the weight of the sample in grams. The number obtained is the concentration of boron in the sample in parts per million (ppm).

The calculation can be shown as:

$$\text{boron concentration} = \frac{\frac{\text{sample (ct/s)}}{\text{std (ct/s)}} - \text{blank (ug)}}{\text{sample weight (g)}}$$

4.7 The Blank Interference

There are three possible sources of background boron produced gamma rays during PGNA. This value needs to be determined in order to increase the accuracy of the analysis, especially for samples with low boron concentration. The possible sources of blank interference are:

- 1) From boron bearing components within the detector and close to the sample position.
- 2) From the sample packaging material (a teflon tube and two polyethylene caps).
- 3) From scattered radiation from nearby boron insulation.

The amount of interference from the blank was determined by irradiating a blank teflon tube with polyethylene caps and recording the emitted prompt gamma ray energy. T.A. Middleton irradiated 18 blanks for 7200 seconds each from May to August 1987. The average value of all the blanks was found as 0.27 ug with a standard deviation 0.12 ug. This is the value of the blank used in the calculation for the concentration of boron.

4.8 Precision of PGNAA

In order to determine the precision of PGNAA, a sample of mid range boron concentration was measured on seven separate analyses. These were performed by Patty Smith during the month of April 1988. The results are presented in table 4.1, and it can be seen that the reproducibility, although not as precise as originally hoped, is still low enough for the purposes of this study.

4.9 Accuracy of PGNAA

Accuracy of the PGNAA system was determined by Ash (1987). Standard NBS-1571, known to have a boron concentration of 33 ppm, was used. An aliquot was irradiated on three separate occasions in an attempt to reproduce the accepted boron concentration. The

accuracy of PGNAAs was determined to be within experimental error, as shown by table 4.2. (after Ash, 1987)

Table 4.1 The Precision of PGNAA

SAMPLE	BORON (ppm)
870825-25	1) 3.15
	2) 2.79
	3) 3.64
	4) 3.38
	5) 2.94
	6) 4.03
	7) 3.89

$$\bar{x} \text{ (ppm)} = 3.40$$

$$\text{Error} = 12.6\%$$

Table 4.2

Boron analysis of NBS-1571 (accepted boron concentration = 33 ppm.) (after Ash 1987)

SAMPLE	IRRADIATION	BORON (ppm)	\bar{x} (ppm)	σ	33ppm- \bar{x}
	1. 1000 s	31.6			
NBS-1571*	2. 1000 s	33.0	32.9	0.976	0.131
	3. 1000 s	34.0			

Note: *U.S. Bureau of Standards

$$\sigma = \sqrt{\frac{\sum x^2 - n\bar{x}^2}{n}}$$

CHAPTER FIVE

INTERPRETATIONS

5.1 Discussion of the Results

The results for the boron concentrations of the samples are presented in table 5.1. The boron concentration in each major rock forming mineral has been shown to be very variable, ranging from 1 ppm in some samples to over 100 in others. The range of boron content in most of the samples is about 5-10 ppm, but many samples vary from this norm. The biotite ranges from 2.83 ppm to 31.6 ppm, the K-feldspar from 5.17 ppm to 78.5 ppm, the plagioclase from 7.88 ppm to 107.1 ppm, hornblende from 5.19 ppm to 37.0 ppm, and the pyroxenes from 1.95 ppm to 36.8 ppm. Also, the results show no preferential partitioning into one specific mineral over another. Preferential partitioning was sought by plotting the boron concentrations in pairs of coexisting minerals against each other, and in doing so examining the distribution coefficient between them. There were sufficient data to plot three distribution curves; plagioclase vs. biotite, hornblende vs. biotite and biotite vs. K-feldspar which are shown as fig. 5.1, 5.2 and 5.3 respectively. Upon examination of figure 5.1 it can be seen that there are two points with relatively similar K_D values. These two points are used to draw a best fit line from the origin, the slope of which representing the K_D of the two minerals. The one distribution coefficient that is not near the other two is from sample 690422-3, which has two minerals that coexisted in an amphibolite grade of metamorphism. The two

TABLE 5.1 The Measured Boron Concentrations of the Samples

SAMPLE	MINERAL	BORON (ppm)	\bar{x} (ppm)	σ
MCC-761	Hornblende Biotite	5.19 2.83 Δ		
MCC-704	Hornblende Biotite	22.13 12.83		
MCC-703	Hornblende Biotite	26.88 6.00 ; 6.04	6.02	0.02
690422-3	Biotite Hornblende Sphene Plagioclase K-Feldspar	2.92 18.35 5.90 ; 8.06 16.99 77.5 ; 79.5 $^{\circ}$	6.98 78.5	1.08 1.00
U-26	K-Felspar Biotite	7.92 5.26		
U-27	Biotite K-Felspar	8.31 ; 7.89 4.83 ; 5.51	8.10 5.17	0.21 0.34
U-70	Hornblende Plagioclase	36.98 $^{\circ}$ 107.1 $^{\circ}$		
U-94	Biotite K-Feldspar Plag. + Quartz	16.86 ; 15.36 13.79 ; 14.64 34.47	16.11 14.21	0.75 0.42
U-115	Biotite K-Felspar	31.65 ; 31.69 11.75 ; 11.86	31.67 11.81	0.02 0.05
U-251	K-Feldspar Biotite Plag. + Quartz	3.29 ; 3.92 2.76 ; 2.96 7.88	3.60 2.86	0.31 0.10
Ca-76	Sphene Hornblende Pyroxene	1.26 16.47 16.18		
Ca-56	Sphene Pyroxene	0.92 16.17		
Ca-65	Fluorite Magnetite + Pyroxene	1.08 26.41		

(continued...)

TABLE 5.1 Continued

SAMPLE	MINERAL (ppm)	BORON (ppm)	\bar{x} (ppm)
Ca-30	Phlogopite	15.78	34.16 ^o
	Pyroxene	34.16	
Ca-105	Diopside	13.93	18.51
	Phlogopite	18.51	
Ca-44a	Pyroxene	29.22	0.71
	Fluorite + (Apatite)	0.71	
ON-10	Biotite	9.46	2.22
	Sphene	2.22	
721104	Magnetite	7.12	11.58
	Biotite	11.58	
	Pyroxene	3.65	
	Orthopyroxene	1.95	

These samples were measured with reference to the boric acid #B7 standard, containing 102 μg of boron.

All samples were irradiated for 1000 seconds except:

- o 500 second irradiation
- Δ 2000 second irradiation

$$\text{Standard Deviation} = \sigma = \sqrt{\frac{\sum x^2 - n\bar{x}^2}{n}}$$

n = number of variables

\bar{x} = mean of n amount of variables

TABLE 5.2 The Distribution Coefficients of Coexisting minerals

SAMPLE	COEXISTING MINERALS	x_B / x_B	K_D	$1/K_D$
MCC-761	Hornblende / Biotite	5.19/2.83	1.83	
MCC-704		22.1/12.8	1.72	
MCC-703		26.9/6.04	4.45	
690422-3		18.3/2.92	6.28	
U-94	Biotite / K- Feldspar	16.1/14.2	1.13	0.88
U-115		31.7/11.8	2.68	0.37
U-251		2.86/3.60	0.79	1.27
U-26		5.26/7.92	0.66	1.51
U-27		8.10/5.17	1.57	0.64
690422-3		2.92/78.8	0.04	25.0
U-251	Biotite / Plagioclase	2.86/7.88	0.36	2.78
U-94		16.1/34.4	0.47	2.13
690422-3		2.92/17.0	0.06	16.7
690422-3	Plagioclase / K-spar	17.0/78.5	0.22	4.54
U-94		34.4/14.2	2.43	0.41
U-251		7.88/3.60	2.19	0.46
Ca-56	Pyroxene / Sphene	16.2/0.92	17.6	
Ca-76		16.2/1.26	12.9	
690422-3	Hornblende / Sphene	18.3/6.98	2.63	
Ca-76		16.4/1.26	13.1	
ON-10	Biotite / Sphene	9.46/2.22	4.26	0.23
690422-3		2.92/8.06	0.36	2.78
690422-3	Plagioclase / Hornblende	17.0/18.3	0.93	1.07
U-70		107/37.0	2.90	0.34
721104	Magnetite / Pyroxene	7.12/3.65	1.95	
	Magnetite/Orthopyroxene	7.12/1.95	3.65	
	Biotite / Pyroxene	11.6/3.65	3.17	
	Biotite / Orthopyroxene	11.6/1.95	5.94	
	Biotite / Magnetite	11.6/7.12	1.63	
	Orthopyroxene/Pyroxene	1.95/3.65	0.53	
Ca-105	Phlogopite / Diopside	18.5/13.9	1.33	0.75
Ca-30	Phlogopite / Pyroxene	15.8/34.2	0.46	2.17
690422-3	Sphene / K-Feldspar	6.98/78.5	0.09	11.1
690422-3	Sphene / Plagioclase	6.98/17.0	0.41	2.44
Ca-65	Mag. + Pyrox. / Fluorite	26.4/1.08	24.5	
Ca-76	Hornblende / Pyroxene	16.5/16.2	1.02	
Ca-44a	Fluorite / Pyroxene	0.71/29.2	0.02	41.7

Plagioclase vs. Biotite

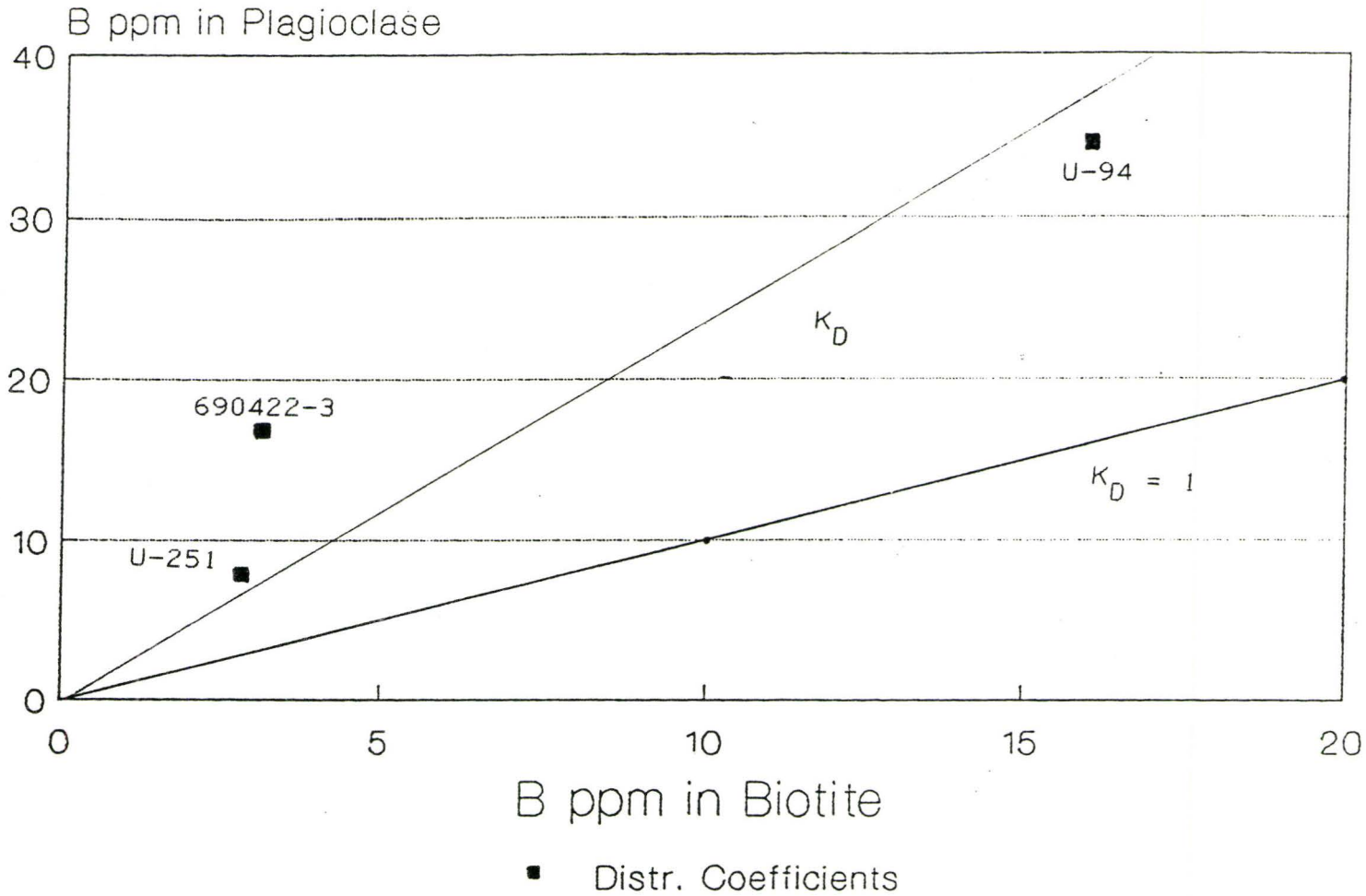


FIGURE 5.1 The plot of the distribution coefficients for plagioclase vs. biotite. (from table 5.2)

Hornblende vs. Biotite

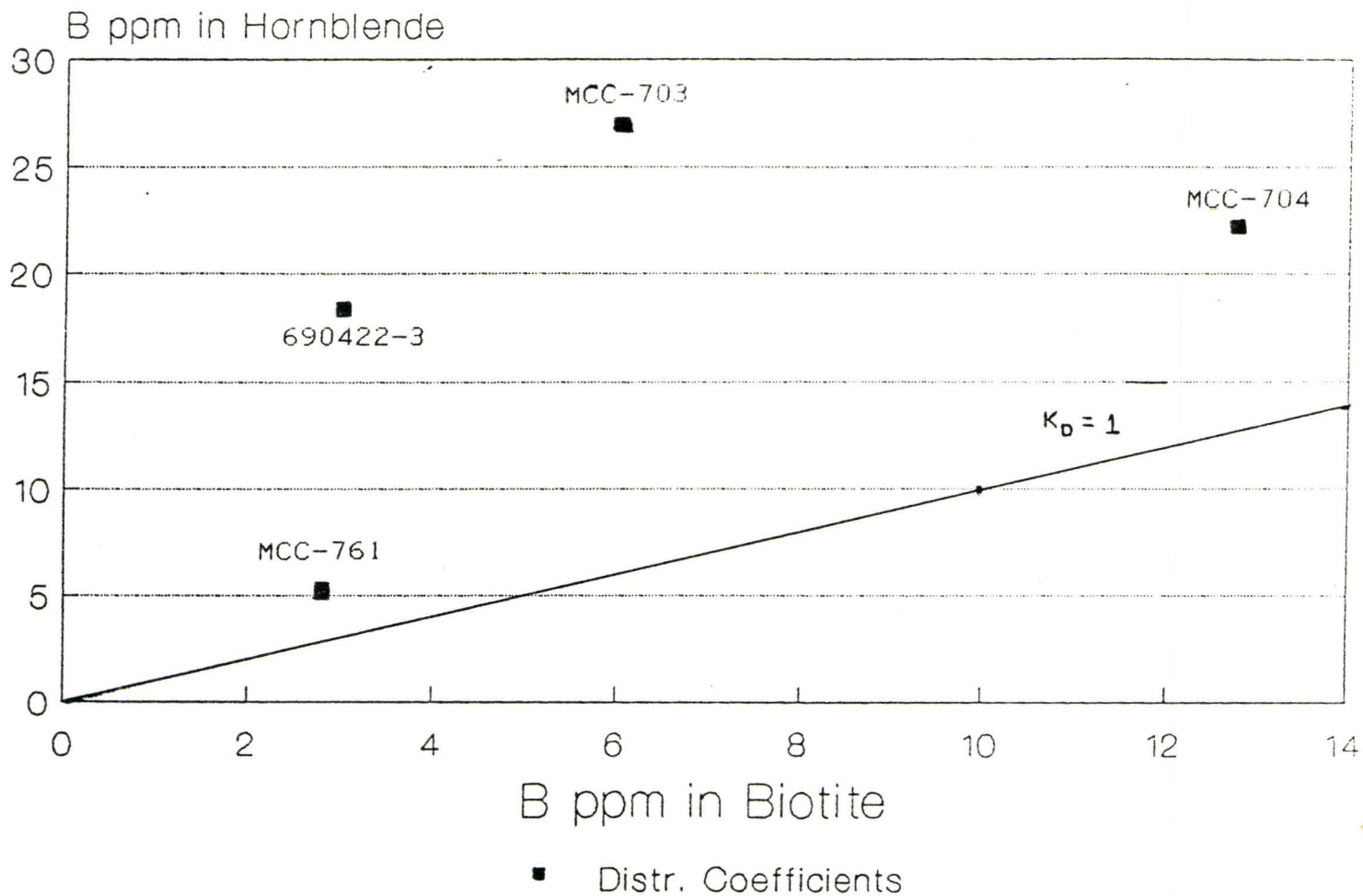


FIGURE 5.2 The plot of the distribution coefficients for hornblende vs. biotite. (from table 5.2)

Biotite vs. Feldspar

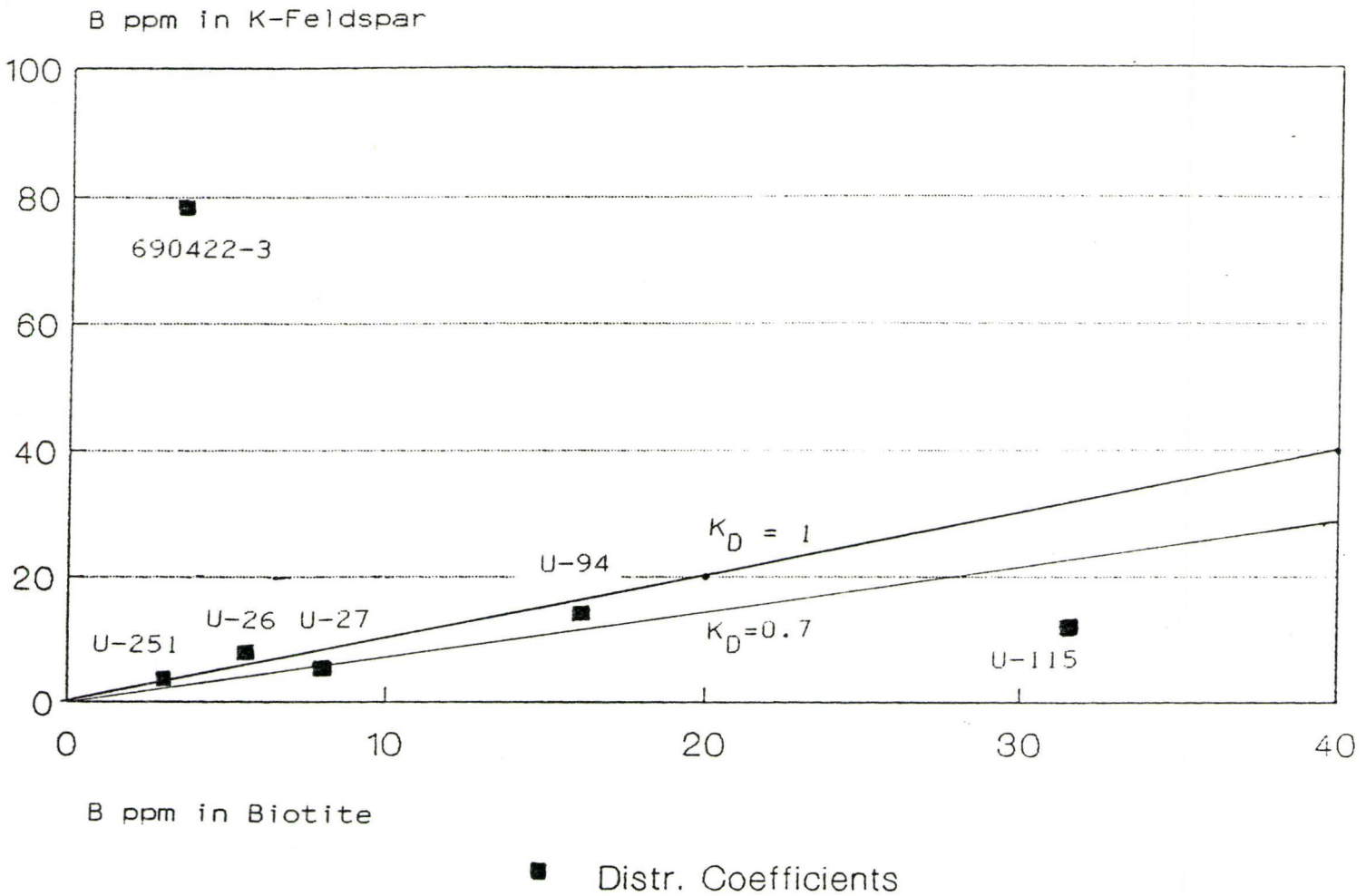


FIGURE 5.3 The plot of the distribution coefficients for biotite vs. K-feldspar. (from table 5.2)

similar distribution coefficients are from samples U-251 and U-94, which originate from igneous sources as monzonites. Figure 5.2 shows four distribution points which produce a scattered plot. The four pairs of coexisting mineral phases in this plot are from samples MCC-761, MCC-704, MCC-703 and 690422-3. The MCC samples are from an almandine amphibolite grade of metamorphism, while 690422-3 is from an unspecified amphibolite rock. Figure 5.3 shows a distribution plot of five points which can fit fairly well along a best fit distribution line originating from the origin (drawn in and labelled as K_D) and one point which does not. The five points which fit according to the curve are all of igneous origin (quartz monzonites and monzonites from the U-series samples) and are all from the same pluton. The one point which does not fit on the line drawn in figure 5.3 is from sample 690422-3, an amphibolite rock. It can be seen in each plot that wherever the distribution coefficients vary, the two coexisting phases originated from a rock of amphibolite grade of metamorphism.

Upon examination of table 5.2, it can be seen that there is a wide range of distribution coefficients among the remaining minerals that were not plotted. There were some minor patterns noticeable, however. For example, the boron concentrations of sphene and fluorite were consistently low compared to the other coexisting minerals. Four sphene samples were measured for boron concentration, 2.8 ppm, while the average boron concentration for fluorite was about 1 ppm.

These studies were carried out on previously crushed samples, and although every precaution for purity was taken, it should be kept in mind that these minerals might have been exposed to some form of boron that might have affected the results, for example a cleaning process. This is improbable, however, not impossible.

5.2 Comparisons and Interpretations

It can be clearly seen from the discussion of the results that the coexisting mineral phases from an igneous source show much less variable distribution coefficients than the coexisting mineral phases from a metamorphic origin. The igneous distribution coefficients did vary somewhat, and due to the limited data available in this study it was not feasible to assign a numerical value for hornblende/biotite (fig. 5.1) and biotite/plagioclase (fig. 5.3). For K-feldspar/biotite, the slope of the best fit line (labelled as K_D) is 0.7. This is the preferential boron partition for K-feldspar/biotite. It can be concluded from this that the coexisting minerals originating from igneous sources did in fact show a preferential boron partition, whereas the minerals originating from metamorphic terrains did not. A good future study might be to attempt to measure the boron partition among coexisting metamorphic minerals that originate from outcrops that vary in metamorphic grade, and in doing so, determine why metamorphic rocks do not show a preferential boron partition. A possible explanation to this

problem may be that the minerals in the metamorphic phase may no longer coexist in equilibrium, causing the ability of one of the mineral phases to incorporate boron complex ions to change with relation to the other.

Most trace elements show selective partitioning into coexisting mineral lattices according to their ionic potentials. As previously mentioned, boron may replace the Al^{3+} ion in feldspars and phyllosilicates. Truscott et al. found that boron has been found to be more abundant in biotite than in amphiboles or plagioclase. This is not been the case here, as biotite has shown very variable concentrations with relation to plagioclase and hornblende, however it was found that boron is preferentially concentrated in biotite over K-feldspar. It was determined by Ahmad et al. (1981), and Truscott et al. (1986) that boron is commonly concentrated in alteration products such as sericite and saussurite. However, very little alteration of any of the grains in the present study could be seen, so it is doubtful that alteration is the cause of any of the high boron concentrations. Shaw et al. (1986) also found boron concentration along the fractures in mineral grains, but very little fracturing or fluid inclusions were found in the present minerals. (see table 3.1)

5.3 Summary

The coexisting mineral phases originating from igneous sources did show a preferential boron partition, which was determined to be 0.7 in K-feldspar/biotite. This conclusion is

derived by determining a best fit line between the plotted points in figures 5.1 and 5.3, the slope of which is the preferential boron distribution between the two mineral phases that define the axis of the graphs. Due to limited data, it was not possible to designate a numerical value for the slope of the line drawn through the distribution points in figure 5.1. The coexisting mineral phases that originate from metamorphic rocks did not show a preferential boron partition, as shown by fig. 5.2.

Sphene and fluorite consistently showed low boron concentrations, especially in comparison with other coexisting mineral phases, such as biotite, pyroxene, hornblende and feldspars. (see table 5.1)

The variable boron concentrations in the major rock forming minerals can not be explained by alteration products such as sericite or saussurite, alteration along fractures of the mineral grains or extensive fluid inclusions.

REFERENCES

- AHMAD, R., and WILSON, C.J.L., 1981. Uranium and boron distributions related to metamorphic fluid activity. *Contrib. Mineral. Petr.*, 76, 24-32
- ASH, J.S., 1987. The concentration and distribution of boron in the Keweenaw Metabasalts of Mamainse Point, Ontario. un pub. B.Sc. thesis, McMaster University, Hamilton, Ontario.
- CARMICHAEL, I.S.E., TURNER, F.J., VERHOOGEN, J., 1974. *Igneous Petrology*. McGraw Hill, Toronto, Ont., 80,81
- CHIANG, M.C., 1965. Element partition between biotite and hornblende in the rocks from the Loon Lake Aureole, Chandos Twp. Ontario., unpub. M.Sc. Thesis, McMaster University, Hamilton, Ontario.
- CHRIST, C.L., and HARDER, H.A., 1978. *Handbook of Geochemistry*, vol 2-1, chap. 5.
- DEER, W.A., HOWIE, R.A., ZUSSMAN, J., 1983. *An Introduction to the Rock Forming Minerals*. Longmans
- DEVORE, G.W., 1955. Crystal Growth and the distribution of elements. *J. Geol.* 63, 471-494
- DOSTAL, J., 1973. *Geochemistry and Petrology of the Loon Lake Pluton, Ont.* un pub. Ph.D Thesis, McMaster University, Hamilton, Ontario.
- FUNG, P.C., 1978. K_b, R_b and Tl distributions between coexisting natural and synthetic rock forming minerals. un pub. Ph.D thesis, McMaster University, Hamilton, Ont.
- FYFE, W.S., 1964. *Geochemistry of Solids: An Introduction*. McGraw Hill inc., Toronto.
- GAST, P.W., 1968. Trace Element fractionation and the origin of alkaline magma types. *Geochem. Cosmochem. Acta* 32, 1057-1086.
- GOLDSCHMIDT, V.M., 1937. Principles of Distribution of Chemical Elements in Minerals and Rocks. *J. Chem. Soc.* 655-673
- _____, 1944. Crystal Chemistry and Geochemistry. *Chem. Prod.* 7 (516), 29-34
- HIGGINS, M.D., TRUSCOTT, M.G., SHAW, D.M., BERGERON M., BUFFET

- G.H., COPELY, J.R.D. and PRESTWICK W.V., 1984. Prompt Gamma Neutron Activation Analysis at the McMaster University Nuclear Reactor. *in* Use and Development of Low and Medium Flux Research Reactors (eds O.K. Harling, L. Clark and P. von der Hardt), 690-697. Supplement to vol. 44 Atomkern-Energie Kerntechnik.
- KRETZ, R., 1959. Chemical study of garnet, biotite and hornblende from gneisses of southern quebec, with emphasis on the distribution of elements in coexisting minerals. *J. Geol.* 67, 371-402
- _____, 1960. The distribution of certain elements among coexisting calcic pyroxenes, calcic amphiboles and biotite in skarns. *Geochim. Cosmochim. Acta* 20, 161-191
- _____, 1961. Some applications to coexisting minerals of variable composition. Examples: orthopyroxene - clinopyroxene and orthopyroxene - garnet. *J. Geol.* 69, 361-387
- MALINKO, S.V., BERMAN, I.B., LISITSYN, A.Y., STOLYAROVA, A.N. 1979. Boron in rock forming minerals based on data from a local radiographic analysis. *Int. Geol. Rev.* 21, 1274-1284
- MASON, B.H., and MOORE, C.B., 1982. Principles of Geochemistry. John Wiley and sons.
- MIDDLETON, T.A., 1987. The Prompt Gamma Neutron Activation Analysis system at McMaster University. Tech Memo 87-1 unpub.
- PACESOVA, M., 1973. K-Rb-Tl Relationships in some gneissic rocks. Un pub. M.Sc. Thesis, McMaster University, Hamilton, Ont.
- PRIGOGINE, I. and DEFAY, R., 1954. Chemical Thermodynamics. Longmans
- RINGWOOD, A.E., 1955a. The principles governing trace element distribution during magmatic crystallization. part I) The influence of electronegativity. *Geochim. Cosmochim. Acta.* 7 189-202
- _____, 1955b. The principles governing trace element behavior during magmatic crystallization. part II) The role of complex formation. *Geochim. Cosmochim. Acta.* 74 242-254
- SHAW, D.M., 1953. The camouflage principle and trace element

- distribution in magmatic minerals. J. of Geol. 61
1151-1166
- _____, 1958. Radioactive Mineral Occurences of the Province of Quebec. Quebec Dept. of Mines, Geological Report 80.
- _____, 1977. Trace element behavior during anatexis. Magma Genisis Bull. 96 189-213
- _____, TRUSCOTT, M.G., GRAY, E.A., and MIDDLETON, T.a., 1988. Boron and lithium in high grade rocks and minerals from Wawa, Kapuskasing region, Ontario. un pub.
- TAUSON, L.V., 1965. Factors in the distribution of the trace elements during the crystallization of magmas. Phys. Chem. Earth. 6 215-246
- TAYLOR, S.R., 1965. The application of trace element data to problems in petrology. Phys. Chem. Earth. 6 133-213
- TENNYSON, C.H., 1963. Eine systematik der borate auf kristallchemisher grundlage. Fortschr. Minral. 41
64
- TRUSCOTT, M.G., SHAW, D.M., CRAMER, J.J., 1986. Boron abundance and localization in granulites and the lower continental crust. Bull. Geol. Soc. Finland 58, part 1, 169-177